

# A multiscale model for the controlled selection process of ovulatory follicles

Nki ECHENIM\*, Michel SORINE and Frédérique CLÉMENT

**Abstract**—The biological meaning of follicular development is to free fertilizable oocytes at the time of ovulation. The selection of ovulatory follicles in mammal ovaries is an FSH-dependent selection process. In this paper, we design a multi-scale model of follicular development, where selection arises from the feedback between the ovaries and the pituitary gland and appeals to control theory concepts. Each ovarian follicle is characterized by a 2D density function giving an age and maturity-structured description of its cell population. The control intervenes in the velocity and loss terms of the conservation law ruling the changes in the density. The numerical outputs of the model, integrated with the finite volume method, are consistent with physiological knowledge.

## I. INTRODUCTION

The development of ovarian follicles is a crucial process for reproduction in mammals, as the biological meaning of folliculogenesis is to free fertilizable oocyte(s) at the time of ovulation. A better understanding of follicular development is both a clinical and zootechnical challenge; it is required to improve the control of anovulatory infertility in women, as well as ovulation rate and ovarian cycle chronology in domestic species.

Within all the developing follicles, very few actually reach the ovulatory size; most of them undergo a degeneration process, known as atresia [1]. The ovulation rate (number of ovulatory follicles) results from an FSH (Follicle Stimulating Hormone)-dependent follicle selection process. FSH acts on the cells surrounding the oocyte, the granulosa cells, and controls both their commitment towards either proliferation, differentiation or apoptosis and their ability to secrete hormones such as estradiol. The whole estradiol output from the ovary is responsible for exerting a negative feedback on FSH release.

The previous mathematical models dealing with follicular development can be split into two main approaches. The first one takes into account the mechanisms underlying follicular development on the cellular and molecular scales, considering separately ovulatory and atretic trajectories. It aims at characterizing and understanding FSH-induced changes in granulosa cells [2], [3] and FSH signal transduction [4]. The other approach is concerned with the process of follicle selection *per se* from the viewpoint of follicular population dynamics [5], [6], [7].

\*Unité de Recherche INRIA Rocquencourt, Domaine de Voluceau, Rocquencourt BP 105, 78153 Le Chesnay Cedex, FRANCE  
 nki.echenim@inria.fr

A phenomenological and macroscopic function separates ovulatory follicular trajectories from atretic ones. Only the best-fitted follicles can survive in an unfavorable, FSH-poor environment.

In this paper, we aim at merging the molecular and cellular mechanistic description introduced by the former approach with the competition process dealt with in the latter. To build such a model, we use both multi-scale modeling and control theory concepts. For each follicle, the cell population dynamics is ruled by a first order conservation law with variable coefficients which describes the changes in age and maturity of the granulosa cell density. A control term representing FSH signal intervenes both in the velocity and loss terms of the conservation law. We distinguish between a local control, specific to each follicle (micro scale), and a global control that results from the ovarian feedback (macro scale).

In Section 2, the physiological mechanisms underlying the model assumptions as well as the model terms are described. Section 3 deals with the numerical simulation of the model equations. The final section discusses the model formulation and future work.

## II. MODEL DESIGN BASED ON CONSERVATION LAWS

### A. Cellular phases

Two types of controls act on the granulosa cells dynamics: one is follicle-specific and operates locally,  $u_f$ , while the other operates globally on the whole ovary,  $U$ .

The granulosa cell population consists of proliferating cells, running along the cell cycle and undergoing mitosis (whereby a mother cell gives birth to two daughter cells), and differentiated cells, having left the cell cycle. Cells may also engage in a dying program, known as apoptosis.

According to biological knowledge, we introduce three main cellular phases:

- Phase 1 corresponds to cells going along the cell cycle but not yet committed to mitosis. A local control term  $u_f$  acts on their maturation and aging velocities. The cells stay in phase 1 until their age (modulo the cell cycle length,  $a_2$ ) reaches the maximum phase age,  $a_1$ , when they enter phase 2, or until their maturity reaches a threshold value,  $\gamma_s$ , when they enter phase 3.
- Phase 2 corresponds to the cells committed to complete the whole cell cycle, whatever the control signal may be.

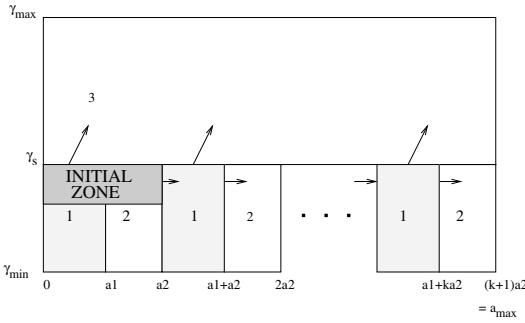


Fig. 1. Cellular phases in the age-maturity plane. The cell cycle consists of the cyclic phase 1-phase 2-phase 1 pathway. When it enters phase 1 from phase 2, a mother cell gives birth to two daughter cells. Cell differentiation corresponds to the one-way flow from phase 1 into phase 3.  $a_2$  is the cell cycle length. Cells in the initial zone are asynchronous in age but quite synchronous in maturity.

They undergo mitosis once their age (modulo the cell cycle length) reaches the maximum phase age,  $a_2$ , when they enter phase 1 once again.

- Phase 3 corresponds to differentiated cells, which have exited the cell cycle in an irreversible way, after their maturity has reached the threshold  $\gamma_s$ . The local control  $u_f$  only acts on their maturation velocity.

Figure 1 illustrates the different phases in the age-maturity plane.

In phase 1 and 3, cells may undergo apoptosis. Such a phenomenon occurs for a specific interval of maturity values, if the global resource in FSH,  $U$ , is poor, compared to a reference value [1].

Populations of numerous cells are commonly described with continuous representations and conservation laws are usually used to describe the dynamics of cell densities (see e.g. [8]). For a given follicle,  $f$ , and cellular phase,  $p$ , we introduce the cell density function  $\phi_f(a, \gamma, t)$ .  $a$  denotes the cell age,  $\gamma$  the cell maturity, and  $t$  denotes time. The generic form of the conservation law for  $\phi_f$  is:

$$\forall a \in [0, +\infty), \quad \forall \gamma \in [0, +\infty) \\ \frac{\partial \phi_f}{\partial t} + \frac{\partial g_{fp}(u_f)\phi_f}{\partial a} + \frac{\partial h_{fp}(\gamma, u_f)\phi_f}{\partial \gamma} = -\lambda_p(\gamma, U)\phi_f \\ \text{for } p = 1, 2, 3$$

The  $g_{fp}$  and  $h_{fp}$  functions are respectively the aging and maturation velocities, and  $\lambda_p$  is the loss term.

The initial conditions for each follicle are given by:

$$\phi_f(a, \gamma, 0) = \Gamma_f(a, \gamma)$$

According to physiological knowledge, we assume that cells are initially not synchronized within the cell cycle, with a quite narrow range of maturity levels, see initial zone on Figure 1.

We have to define transfer conditions at each phase transition i.e. when the age  $a[a_2]$ <sup>1</sup> switches from  $a_1^-$  to  $a_1^+$ , or from  $a_2^-$

to  $a_2^+(= 0^+)$ , or when the maturity  $\gamma$  overpasses  $\gamma_s$ . As we use conservation laws, the continuity condition is expressed on the fluxes so that:

$$\begin{aligned} \lim_{a[a_2] \rightarrow a_1^+} g_{f2}\phi_f(a, \gamma, t) &= \lim_{a[a_2] \rightarrow a_1^-} g_{f1}\phi_f(a, \gamma, t) \\ \lim_{\gamma \rightarrow \gamma_s^+} h_{f3}\phi_f(a, \gamma, t) &= \lim_{\gamma \rightarrow \gamma_s^-} h_{f1}\phi_f(a, \gamma, t) \\ \lim_{a[a_2] \rightarrow a_2^+} g_{f1}\phi_f(a, \gamma, t) &= \lim_{a[a_2] \rightarrow a_2^-} 2g_{f2}\phi_f(a, \gamma, t) \end{aligned}$$

The boundary conditions on the borders  $a=0$  and  $\gamma=0$  are of Neumann type.

## B. Feedback terms

We define the observation operator:

$$M(\phi_f)(t) = \int \gamma \int \phi_f(a, \gamma, t) da d\gamma \quad (1)$$

This ( $a$  zeroth-order,  $\gamma$  first-order) moment of  $\phi_f$  corresponds to the global maturity in a follicle. Applying the same operator to  $\phi = \sum_f \phi_f$  gives the global maturity in the ovary  $M(\phi)$ .

The global control term  $U$  is a decreasing function of  $M(\phi)$  due to the negative feedback exerted by the ovaries on the secretion of FSH [9]. Its dynamics can be described classically as:

$$\frac{dU(M)(\phi)(t)}{dt} = S[M(\phi)] - kU[M(\phi)] + U_0(t) \quad (2)$$

$S[M(\phi)]$  is a decreasing sigmoid function of  $M(\phi)$  representing FSH release.  $kU[M(\phi)]$  is the clearance of FSH and  $U_0(t)$  represents a potential exogenous entry in FSH.

As  $U$  is a slow variable (compared to the micro variables) we can use the quasi-steady state approximation to reduce the control function:

$$U(M)(\phi) = U_{min} + \frac{U_{max} - U_{min}}{1 + \exp[c(M(\phi) - m)]} \equiv S'(M) \quad (3)$$

$U_{max}$  and  $U_{min}$  are the sigmoid asymptotes,  $m$  the abscissa of its inflection point and  $c$  the slope at this point.

The local control term  $u_f$  is proportional to  $U$ , depending on follicular maturity [10].

$$\begin{aligned} u_f[M(\phi_f), M(\phi)] &= b_f[M(\phi_f)]U[M(\phi)] \\ b_f &\leq 1 \end{aligned}$$

The ovarian system, studied in closed loop, is illustrated on Figure 2.

## C. Velocity and loss terms

In phase 1, the aging velocity is related to the local control  $u_f$ ; it speeds up with increasing values of  $u_f$  [11], [12]. As we had no information on its shape, we used a simple linear formulation:

$$g_{f1}(u_f) = g_1 u_f + g_2$$

<sup>1</sup>[ $a_2$ ] means modulo  $a_2$

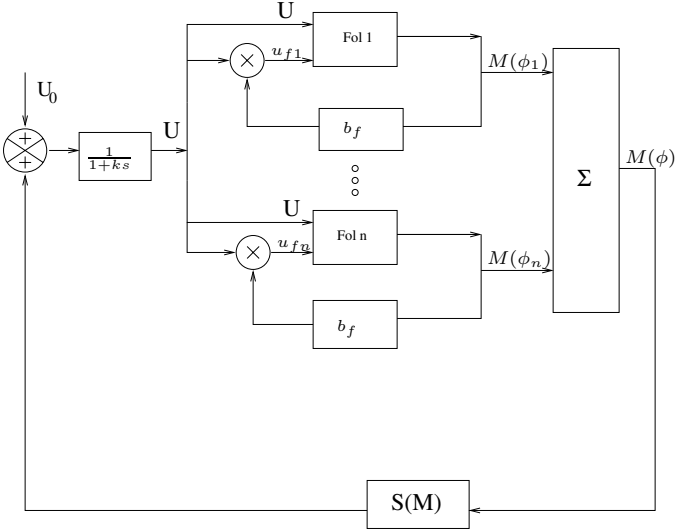


Fig. 2. The ovarian system in closed loop. The global feedback-designed control  $U$  is modulated on the follicle scale ( $Fol_i$ ), through the follicular maturity,  $M(\phi_i)$  to define the operating control  $u_{fi}$ .

In the other phases, age changes like time:  $g_{f2} = g_{f3} = 1$

In phases 1 and 3, the maturation velocity, accounting for the change in the cell responsiveness to FSH speeds up with increasing values of  $u_f$ . The expression for the maturation velocity was inspired from a previous study [4]. We retained the following simplified equation ruling the changes of  $\gamma$ :

$$h_{f1} = h_{f3} = \beta \left( \frac{k_1}{1 + \frac{\gamma k_2}{\delta + \gamma} (k_3 + \frac{1}{k_4 u_f})} - \gamma \right) \gamma$$

In phase 2, the maturity remains unchanged :  $h_{f2} = 0$ .

In phases 1 and 3, the apoptosis entry rate, denoted by  $\lambda_i$ , is assumed to depend both on the cell maturity level and the level of FSH supply:

$$\lambda_i(\gamma, U) = \bar{\lambda}_i \omega(\gamma) \frac{|U_{max} - U|_-}{U_{max}} \quad i = 1, 2, 3$$

where  $\omega(\gamma)$  is a Gaussian function centered on  $\gamma_s$ , and  $|x|_- = \frac{1}{2}(|x| - x)$ .

In phase 2, cells are not vulnerable to apoptosis so that  $\lambda_2 = 0$ .

#### D. Model summary

The whole model can be summarized by the global conservation law:

$$\begin{aligned} \forall a &\in [0, +\infty), \forall \gamma \in [0, +\infty) \\ \frac{\partial \phi_f}{\partial t} + \frac{\partial g_{fp}(u_f)\phi_f}{\partial a} + \frac{\partial h_{fp}(\gamma, u_f)\phi_f}{\partial \gamma} &= -\lambda_p(\gamma, U)\phi_f \\ \text{For } p &= 1, 2, 3 \end{aligned} \quad (4)$$

with  $p = 1$  if  $a[a_2] \in [0, a_1], \gamma \in [0, \gamma_s]$  and

$$\begin{aligned} g_{f1} &= g_1 u_f + g_2 \\ h_{f1} &= \beta \left( \frac{k_1}{1 + \frac{\gamma k_2}{\delta + \gamma} (k_3 + \frac{1}{k_4 u_f})} - \gamma \right) \gamma \\ \bar{\lambda}_1 &= 1 \end{aligned}$$

$p = 2$  if  $a[a_2] \in ]a_1, a_2], \gamma \in [0, \gamma_s]$  and

$$\begin{aligned} g_{f2} &= 1 \\ h_{f2} &= 0 \\ \bar{\lambda}_2 &= 0 \end{aligned}$$

$p = 3$  if  $a \in [0, +\infty), \gamma \in [\gamma_s, +\infty)$  and

$$\begin{aligned} g_{f3} &= 1 \\ h_{f3} &= \beta \left( \frac{k_1}{1 + \frac{\gamma k_2}{\delta + \gamma} (k_3 + \frac{1}{k_4 u_f})} - \gamma \right) \gamma \\ \bar{\lambda}_3 &= 1 \end{aligned}$$

Ovulation is triggered as soon as the ovarian maturity reaches a threshold  $M_s$  so that at ovulation time  $T$

$$M(\phi)(T) = M_s$$

The follicles are then sorted; the ovulatory follicles are those whose maturity has overcome a threshold [13]

$$M(\phi_f)(T) \geq M_{fs}$$

$N = Card\{f / M(\phi_f)(T) \geq M_{fs}\}$  is thus the ovulation rate. For any fixed  $N$  and  $T$  values, this defines an accessibility problem starting from given initial conditions and parameter values. A further control problem consists in modifying the expected ovulation rate and/or ovulation time by a suitable control law thanks to the  $U_0(t)$  term.

## III. NUMERICAL SIMULATIONS

### A. Numerical calibration

Even if the framework of the model applies for most mammalian species, the numerical simulation is dedicated to the ovine species. This species is indeed particularly interesting regarding the follicle selection process, as the ovulation rate in the ewe may vary from one to more than six follicles. The numerical calibration called as much as possible for data available in the literature. When no data was available, an heuristic identification was undergone, so that the simulation outputs in terms of cell number fitted desired outputs. The values of the parameters are summarized in Table I.

### B. Numerical scheme

The model handles conservation laws, and more precisely, variable-coefficient with nonlinear source term equations. The finite volume method is the most appropriate to solve such equations numerically. In this framework, we used the BEARCLAW (Boundary Embedded Adaptive Refinement Conservation LAW package)<sup>2</sup> software. It is based on an

<sup>2</sup><http://www.amath.unc.edu/Faculty/mitran/bearclaw.html>

	Parameters	Definition/Nominal value
$U[M(t)]$	$U_{max}$	maximal FSH plasmatic value: $3ng/ml$
	$U_{min}$	minimal FSH plasmatic value: $1.5ng/ml$
	$c$	slope parameter: $2mo^{-1}$
	$m$	abscissa of the inflection point: $4.5mo$
$g_f(u_f)$	$g_1$	slope parameter: $80ml/(ng.s)$
	$g_2$	origin ordinate: $0.7s^{-1}$
$h_f(\gamma, u_f)$	$\beta$	time scale parameter: $0.7mo^{-1}s^{-1}$
	$k_1$	degree of FSH signal amplification: $2.2mo$
	$k_2$	Hill function saturation parameter: $0.6d$
	$\delta$	Hill function half-saturation parameter: $0.26mo$
	$k_3$	recycling rate of FSH receptors: $40nd$
	$k_4$	FSH binding rate: $0.15ml/ng$
Domain length	$a_0$	cell age at the beginning of phase 1: $0 cc$
	$a_1$	cell age at the beginning of phase 2: $0.5 cc$
	$a_2$	cell age at the end of phase 2: $1 cc$
	$a_{max}$	maximal cell age in phase 3: $8 cc$
Domain height	$\gamma_{min}$	minimal maturity in phases 1 and 2: $0mo$
	$\gamma_s$	maturity threshold for cell cycle exit: $0.3mo$
	$\gamma_{max}$	maximal maturity level in the phase 3: $0.7mo$
Ovulation thresholds	$M_s$	ovarian threshold for ovulation triggering: $4.5 \times 10^6 mo$
	$M_{fs}$	follicular threshold for ovulation ability: $2 \times 10^6 mo$

TABLE I

MODEL PARAMETERS:  $mo$  represents the number of molecules (unit:  $10^4$ ), "d" means dimensionless, "cc" means cell cycle.

approximation of the integral of the solution over a “finite volume”, representing the subdivision of the spatial domain into intervals along the age and maturity axis.

We rewrite equation (4) in a non-conservative way:

$$\begin{aligned} \frac{\partial \phi_f}{\partial t} + g_{fp}(u_f) \frac{\partial \phi_f}{\partial a} + h_{fp}(\gamma, u_f) \frac{\partial \phi_f}{\partial \gamma} \\ = -\lambda_p(\gamma, U)\phi_f - \frac{\partial h_{fp}(\gamma, u_f)}{\partial \gamma}\phi_f \\ \equiv -\alpha(\gamma, u_f, U)\phi_f \end{aligned}$$

In the algorithm, each phase  $p$  was distinguished by position-dependent (in  $a$  and  $\gamma$ ) velocities and loss terms, which allows for computing a scalar conservation law rather than a system of conservation laws.

This equation is computed by means of a fractional-step method with Godunov splitting, where  $\phi_f^*(t)$  would be the solution at time  $t$  of the equation without source term:

$$\frac{\partial \phi_f^*}{\partial t} + g_{fp}(u_f) \frac{\partial \phi_f^*}{\partial a} + h_{fp}(\gamma, u_f) \frac{\partial \phi_f^*}{\partial \gamma} = 0 \quad (5)$$

$$\frac{\partial \phi_f}{\partial t} = -\alpha(\gamma, u_f, U)\phi_f^* \quad (6)$$

In the scalar case, this splitting does not introduce numerical error [14]. Let  $Q_{ij}^n$  be an approximation of the average solution to (5) on the finite volume  $C_{ij}$ :

$$Q_{ij}^n \equiv \frac{1}{\Delta a} \frac{1}{\Delta \gamma} \int_{C_{ij}} \phi(a, \gamma, t_n) da d\gamma$$

At the first step of the algorithm,  $Q_{ij}^0$  is a discretization of the initial distribution  $\Gamma_f(a, \gamma)$ . Then, at each time step, the values of the solution on the finite volumes are updated, using approximations to the flux through the endpoints of the volumes. The solution to (5) is computed according to the DCU (Donor-Cell Upwind) algorithm, which takes into account the normal fluxes of the solution:

$$\begin{aligned} Q_{ij}^{n+1} = Q_{ij}^n & - \frac{\Delta t}{\Delta a} (A^+ \Delta Q_{i-\frac{1}{2},j}^n + A^- \Delta Q_{i+\frac{1}{2},j}^n) \\ & - \frac{\Delta t}{\Delta \gamma} (B^+ \Delta Q_{i,j-\frac{1}{2}}^n + B^- \Delta Q_{i,j+\frac{1}{2}}^n) \end{aligned}$$

Let  $g_{ij}^\pm$  and  $h_{ij}^\pm$  be respectively the aging and maturation velocities on the finite volumes (we remove the  $f$  subscript for convenience and consider the velocity sign explicitly). These fluctuations are defined as:

$$\begin{aligned} A^\pm \Delta Q_{i \pm \frac{1}{2}, j}^n &= g_{i \pm \frac{1}{2}, j}^\pm (Q_{ij}^n - Q_{i-1,j}^n) \\ B^\pm \Delta Q_{i,j \pm \frac{1}{2}}^n &= h_{i,j \pm \frac{1}{2}}^\pm (Q_{ij}^n - Q_{i,j-1}^n) \end{aligned}$$

This method gives a first order accuracy which can be improved by adding correction fluxes,  $\tilde{F}$  and  $\tilde{G}$ , to the approximated solution, to take into account the transverse fluxes (i.e the contribution of the  $Q_{i \pm 1, j \pm 1}^n$  terms into the updating of  $Q_{ij}^{n+1}$ ) according to the CTU (Corner-Transport Upwind) method (see the Appendix for details).

Then the solution to (6) is computed:

$$Q_{ij}^{n+1} = Q_{ij}^n \exp \left( - \int_{t_n}^{t_{n+1}} \alpha_{ij}^n dt \right)$$

### C. Simulation results

We simulated a “competition” process between two follicles with the same initial conditions but different sensitivity parameters. The cell densities evolve on the domain represented in Figure 1 with  $k = 7$ , and the parameter values are those displayed in Table I. Figure 3 illustrates the simulation outputs, on the ovarian (global maturity) as well as follicular (cell number and follicular maturity) scales. One of the follicles follows an ovulatory trajectory, while the other follows an atretic trajectory. The ovulatory trajectory is characterized by an increase in the

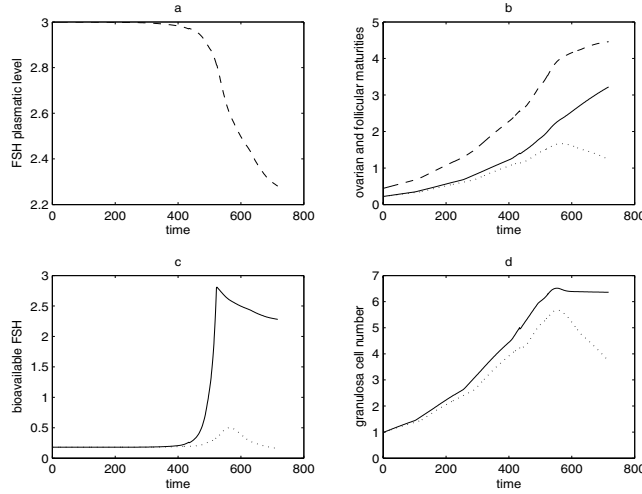


Fig. 3. Selection process within a cohort of 2 follicles. Dashed lines correspond to ovarian scale outputs, solid lines correspond to follicle 1 ( $\beta = 0.7$ ), dotted lines to follicle 2 ( $\beta = 0.6$ ). Panel (a): FSH plasmatic level,  $U$ , Panel (b): ovarian and follicular maturities, Panel (c): bioavailable FSH,  $u_f$ , Panel (d): number of granulosa cells (unit is  $10^6$ ). Time unit: 100 corresponds to 1 cell cycle. Follicle 1 follows an ovulatory trajectory, follicle 2 an atretic one.

number of cells from 1 million to 6.5 million in about 6 cell cycles. The results highlight the effect of the local control, which confines the cells of the atretic follicle in the area of vulnerability towards apoptosis, whereas it allows the cells from the other follicle to escape from this area.

We also studied the effect of altering the sensitivity of FSH release to ovarian feedback ( $m = 3$ ). Figure 4 illustrates a case of high sensitivity to ovarian feedback, leading to a premature fall in the global control  $U$ . None of the follicles resist to this fall, and the ovarian maturity  $M(\phi)$  fails to reach the threshold to trigger ovulation, which results in an anovulatory situation.

We have also investigated the effect of adding exogenous FSH. We first simulated the selection process within a five follicle cohort with different initial conditions and velocity parameters. The resulting ovulation rate was two. In a next simulation using same initial conditions and parameter values, the fall in FSH was compensated by an exogenous entry  $U_0$ . The resulting ovulation rate became three, as one of the former atretic follicles had been rescued by the exogenous entry.

#### IV. CONCLUSION

We designed a model for the FSH-controlled process of ovulatory follicle selection. As in physiological situations where the ovulatory follicles can not be differentiated within the cohort a follicle is not predestined to ovulate in our model. Indeed, the selection process results from the interaction between the follicles' dynamics (depending

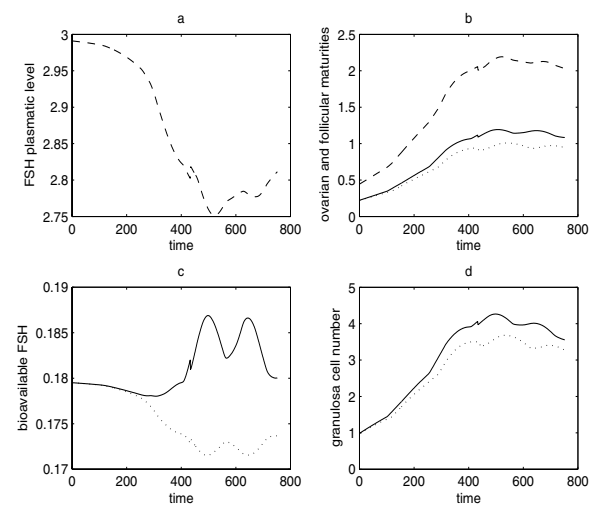


Fig. 4. Selection process in case of a high control sensitivity to feedback. Dashed lines correspond to ovarian scale outputs, solid lines correspond to follicle 1 ( $\beta = 0.7$ ), dotted lines to follicle 2 ( $\beta = 0.6$ ). Panel (a): FSH plasmatic level,  $U$ , Panel (b): ovarian and follicular maturities, Panel (c): bioavailable FSH,  $u_f$ , Panel (d): number of granulosa cells (unit is  $10^6$ ). Time unit: 100 corresponds to 1 cell cycle. Both trajectories are anovulatory.

on initial conditions and sensitivity parameter values) and the hormonal environment dynamics (depending on initial FSH level and feedback exerted by the whole follicular population). The main control operates on the micro scale, in a follicle-specific manner, while the feedback law issues from a macro scale information, defined on the ovary level. The two-way interaction between the micro and macro scales calls for the moments of the density function. Our approach thus merges the mechanistic viewpoint focusing on FSH effects on granulosa cells, with the population dynamics viewpoint focusing on the ovarian-mediated interactions between follicles.

The model behavior, as assessed by numerical simulations, is consistent with physiological knowledge, regarding (i) the part of the control local modulation in determining the follicle fate (ovulatory or atretic) and (ii) the part of the sensitivity of FSH release to ovarian feedback in determining the ovulation output (mono-, poly- or anovulation). The trial simulation with exogenous FSH administration suggests that a finely tuned FSH control may be used to reach an *a priori* prescribed ovulation rate.

Further work will consist in analyzing the model and solving the associated accessibility and control problems. To this end, the method of characteristics seems promising. Indeed, as the local and global control terms appear in the velocity and loss terms of the conservation law, the solution starting from a given initial condition follows a characteristic curve that can be deformed by the control terms to enter into or escape from definite areas of the  $(a, \gamma)$  plane or to hit a prescribed line in this plane.

A methodic exploration of the physiological and pathological situations allowed by the model for different parameter

configuration and threshold ordering will also be undergone.

## REFERENCES

- [1] G.S. Greenwald and S.K. Roy. Follicular development and its control. In E. Knobil and J.D. Neill, editors, *The Physiology of Reproduction*, pages 629–724. Raven Press, New York, 1994.
- [2] F. Clement, M.-A. Gruet, P. Monget, M. Terqui, E. Jolivet, and D. Monniaux. Growth kinetics of the granulosa cell population in ovarian follicles: an approach by mathematical modelling. *Cell Prolif.*, 30:255–270, 1997.
- [3] F. Clement. Optimal control of the cell dynamics in the granulosa of ovulatory follicles. *Math. Biosci.*, 152:123–142, 1998.
- [4] F. Clement, D. Monniaux, J. Stark, K. Hardy, J-C Thalabard, S. Franks, and D. Claude. Mathematical model of fsh-induced camp production in ovarian follicles. *Am. J. Physiol. (Endocrinol. Metab.)*, 281:E35–E53, 2001.
- [5] H.M. Lacker and E. Akin. How do the ovaries count? *Math. Biosci.*, 90:305–332, 1988.
- [6] A. Chavez-Ross, S. Franks, H.D. Mason, K. Hardy, and J. Stark. Modelling the control of ovulation and polycystic ovary syndrome. *J. Math Biol.*, 36:95–118, 1997.
- [7] J.-C. Thalabard, G. Thomas, and M. Methivier. The emergence of the dominant ovarian follicle in primates: A random driven event? In A. Goldbeter, editor, *Cell to Cell Signalling: From Experiments to Theoretical Models*, pages 387–393. Academic Press, 1989.
- [8] S.I. Rubinow. A maturity-time representation for cell populations. *Biophys. J.*, 8:1055–1073, 1968.
- [9] G.E. Mann, B.K. Campbell, A.S. McNeilly, and D.T. Baird. The role of inhibin and oestradiol in the control of fsh secretion in the sheep. *J. Endocrinol.*, 133:381–391, 1992.
- [10] K.P. McNatty, M. Gibb, D. Dobson, D.C. Thurley, and J.K. Findlay. Changes in the concentration of gonadotropin and steroid hormones in the antral fluid of ovarian follicle throughout the oestrous cycle of the sheep. *Aust. J. Biol. Sci.*, 34:67–80, 1981.
- [11] M.C. Rao, A.R. Midgley Jr, and J.S. Richards. Hormonal regulation of ovarian cellular proliferation. *Cell*, 14:71–78, 1978.
- [12] R.L. Robker and J.S. Richards. Hormone-induced proliferation and differentiation of granulosa cells: a coordinated balance of the cell cycle regulators cyclin d2 and p27kip1. *Mol. Endocrinol.*, 12:924–940, 1998.
- [13] R.J. Scaramuzzi, N.R. Adams, D.T. Baird, B.K. Campbell, J.A. Downing, J.K. Findlay, K.M. Henderson, G.B. Martin, K.P. McNatty, A.S. McNeilly, and C.G. Tsonis. A model for follicle selection and the determination of ovulation rate in the ewe. *Reprod. Fertil. Dev.*, 5:459–478, 1993.
- [14] R. J. Leveque. *Finite volume methods for hyperbolic problems*. Cambridge university press, 2002.

## V. APPENDIX

The expression of the fluxes after adding transverse contribution amounts to:

$$\begin{aligned}
 \tilde{F}_{i-\frac{1}{2},j-1} &= -\frac{1}{2} \frac{\Delta t}{\Delta y} g_{i-\frac{1}{2},j-1}^- h_{i,j-\frac{1}{2}}^- (Q_{ij} - Q_{i,j-1}) \\
 \tilde{F}_{i+\frac{1}{2},j-1} &= -\frac{1}{2} \frac{\Delta t}{\Delta y} g_{i+\frac{1}{2},j-1}^+ h_{i,j-\frac{1}{2}}^- (Q_{ij} - Q_{i,j-1}) \\
 \tilde{F}_{i-\frac{1}{2},j} &= -\frac{1}{2} \frac{\Delta t}{\Delta y} g_{i-\frac{1}{2},j}^- h_{i,j-\frac{1}{2}}^+ (Q_{ij} - Q_{i,j-1}) \\
 \tilde{F}_{i+\frac{1}{2},j} &= -\frac{1}{2} \frac{\Delta t}{\Delta y} g_{i+\frac{1}{2},j}^+ h_{i,j-\frac{1}{2}}^+ (Q_{ij} - Q_{i,j-1}) \\
 \tilde{G}_{i-1,j-\frac{1}{2}} &= -\frac{1}{2} \frac{\Delta t}{\Delta x} h_{i-1,j-\frac{1}{2}}^- g_{i-\frac{1}{2},j}^- (Q_{ij} - Q_{i-1,j}) \\
 \tilde{G}_{i-1,j+\frac{1}{2}} &= -\frac{1}{2} \frac{\Delta t}{\Delta x} h_{i-1,j+\frac{1}{2}}^+ g_{i-\frac{1}{2},j}^+ (Q_{ij} - Q_{i-1,j}) \\
 \tilde{G}_{i,j-\frac{1}{2}} &= -\frac{1}{2} \frac{\Delta t}{\Delta x} h_{i,j-\frac{1}{2}}^- g_{i-\frac{1}{2},j}^+ (Q_{ij} - Q_{i-1,j}) \\
 \tilde{G}_{i,j+\frac{1}{2}} &= -\frac{1}{2} \frac{\Delta t}{\Delta x} h_{i,j+\frac{1}{2}}^+ g_{i-\frac{1}{2},j}^+ (Q_{ij} - Q_{i,j-1})
 \end{aligned}$$